Report of the National Research Center for Disaster Prevention, No. 7, November 1971

551.466:551.465.7:551.556.8(265.5)

Similarity of the Spectral Form of Wind Waves in Earlier Stages of Their Development

By

Noriyuki Iwata

Hiratsuka Branch, National Research Center for Disaster Prevention

Abstract

The developments of surface waves caused by a wind which suddenly begins to blow over a large fetch are observed with a capacitance-type wave gauge. The variation of power spectrum in these transient stages is examined from the viewpoint of dimensional analysis.

It is concluded that the spectral forms are similar to each other in the whole stages of development except in the first few hours when the optimum period of spectrum is smaller than 3.0 sec.

Functional forms of the wave spectra in the so-called equilibrium range could be found by dimensional reasoning at first by Phillips (1958), and systematic application of the similarity consideration to the ocean surface waves of the whole frequencies is carried out by Kitaigorodski (1961).

In the present article it is shown that the spectral forms are similar to each other in the whole stages of development except in the few cases at earlier stages, based on the dimensional reasoning and on the empirical formula of Mitsuyasu (1969) concerning optimum frequency of spectrum.

1. The development of the spectrum of surface waves

In general we may put

$$S=\Phi(f,\ F,\ \tau,\ U,\ g),$$

where S: frequency power spectrum density, f: frequency, F: fetch, τ: duration of wind, U: mean wind velocity at definite height, g: gravity acceleration.

From dimensional reasoning it follows immediately that

$$\frac{Sf^5}{g^2}=\Psi(f_*,\ t_*,\ F_*), \tag{1}$$

where

$$f_*=\frac{fU}{g},\quad t_*=\frac{g\tau}{U}\quad\text{and}\quad F_*=\frac{gF}{U^2}$$

respectively show nondimensional frequency, duration and fetch. In the case of narrow spectrum, the dynamic equivalence between fetch and duration is approximately given by the expressions:

$$\tau=\int_0^F\frac{\mathrm{d}x}{c_m},\quad c_m=\frac{1}{2}\frac{g}{\sigma_m}, \tag{2a, b}$$

where c_m denotes the group velocity of optimum frequency component which is given by the expression (2b) for deep water waves, and $\sigma_m(=2\pi f_m)$ angular frequency. The expression (2a) can be normalized as

$$t_*=4\pi\int_0^{F_*}\frac{f_mU}{g}\mathrm{d}F_*\,. \tag{3}$$

From experiments in wind-water tunnel and also from field observations we have approximately (Mitsuyasu, 1969)

$$\frac{f_mU}{g}=AF_*^{-1/3},\quad A=\left(\frac{U}{u_*}\right)^{1/3}\simeq 3.0\,, \tag{4}$$

so that from (3) we get

$$t_*=6\pi AF_*^{2/3}\,. \tag{5}$$

When the duration of wind is smaller than t_*, we can regard fetch as infinite, for example, for $U=10$ m/sec and $F=50$ km we have equivalent duration of mean wind, $\tau=4.4$ hours, so that the initial stage of development in the first 4 hours is influenced only by duration, fetch being regarded as infinite even if it is limited to 50 km.

In almost all the cases of the initial stage we can thus neglect the contribution of fetch, and then it follows from (1) that

$$\frac{Sf^5}{g^2}=\Psi_1(f_*,\ t_*)\,. \tag{6}$$

Auto-covariance function is defined as follows:

$$C(\tau)=2\int_0^\infty S(f)\cos 2\pi f\tau\mathrm{d}f\,. \tag{7}$$

Substituting (6) into (7), we obtain

$$C(0)=2\frac{U^4}{g^2}\Phi(t_*)\,, \tag{8}$$

where

$$\Phi(t_*)=\int_0^\infty f_*^{-5}\Psi_1(f_*,\ t_*)\mathrm{d}f_*\,.$$

When we denote optimum frequency of power spectrum as f_m, then it follows that

$$\frac{f_mS(f)}{C(0)/2}=\left(\frac{f_mU}{g}\right)^{-4}\left(\frac{f}{f_m}\right)^{-5}\frac{\Psi_1(f_*,\ t_*)}{\Phi(t_*)}\,. \tag{9}$$

Now that from (4) and (5)

$$\frac{f_mU}{g}=Q(t_*),\quad Q^2=6\pi-\frac{A^3}{t_*}\,,$$

we have finally

$$\frac{f_mS(f)}{C(0)/2}=\left(\frac{f}{f_m}\right)^{-5}\frac{\Psi_1[t_*,\ (f/f_m)Q(t_*)]}{\Phi(t_*)Q^4(t_*)}\,. \tag{10}$$

For $t_*\to\infty$, Q and Ψ_1 become asymptotically constant so that the right-hand side of (10) becomes a function of f/f_m. Mitsuyasu (1968) has pointed out that non-dimensional power density of optimum frequency component remains practically constant and does not depend on the fetch,

$$\frac{f_mS(f_m)}{C(0)/2}=\text{constant}.$$

The above relation is confirmed from experiments in wind-water tunnel as well as from field observations in Hakata Bay of the Japan Sea. All data are acquired from wave fields of steady state and limited fetch. When we replace in (10) t_* by F_*, then we obtain a general representation of nondimensional spectrum for the case of steady state and limited fetch, so that the right-hand side of (10) can be regarded practically as independent of t_*.

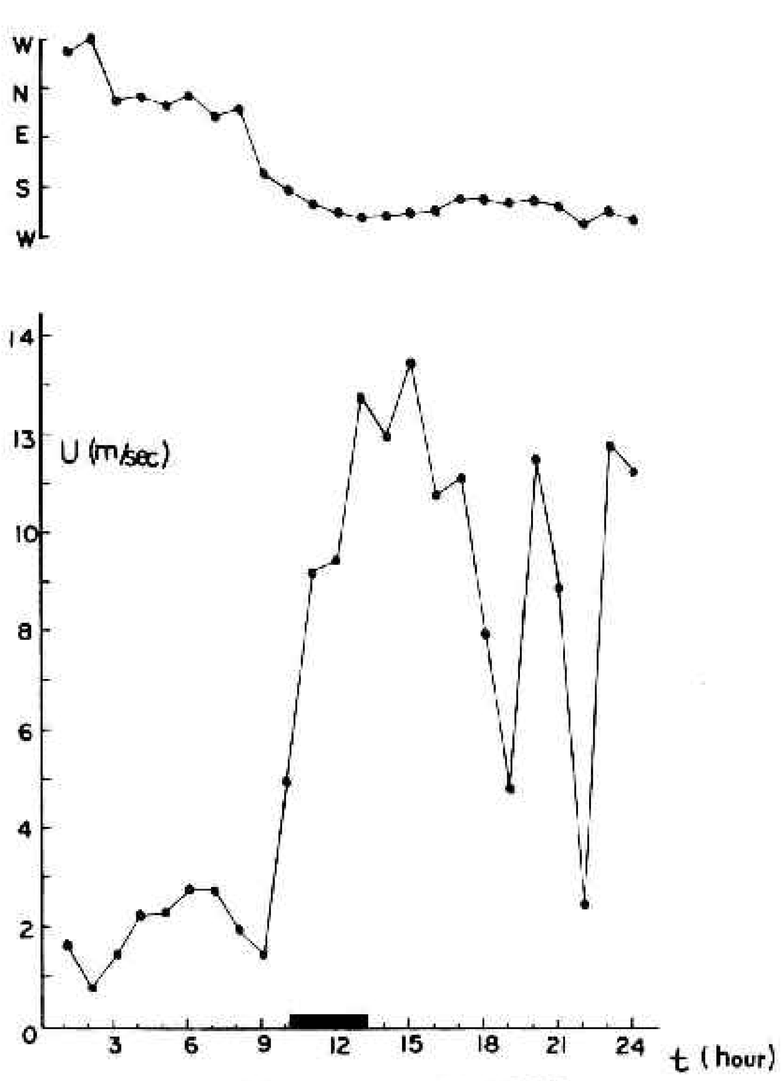

(1) 8 April 1969

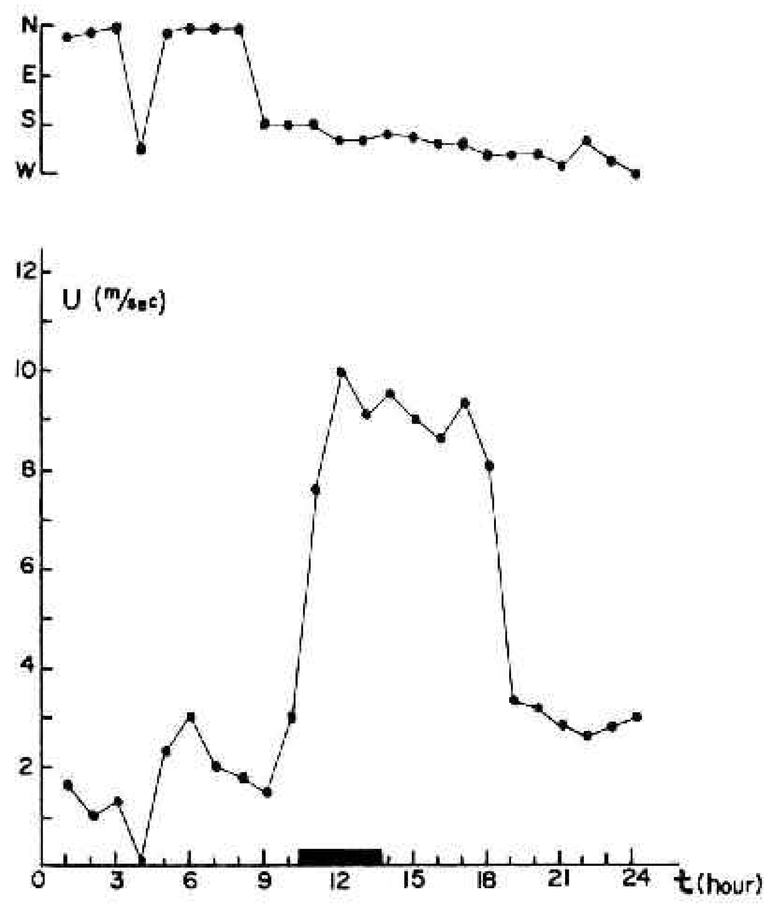

(2) 12 April 1969

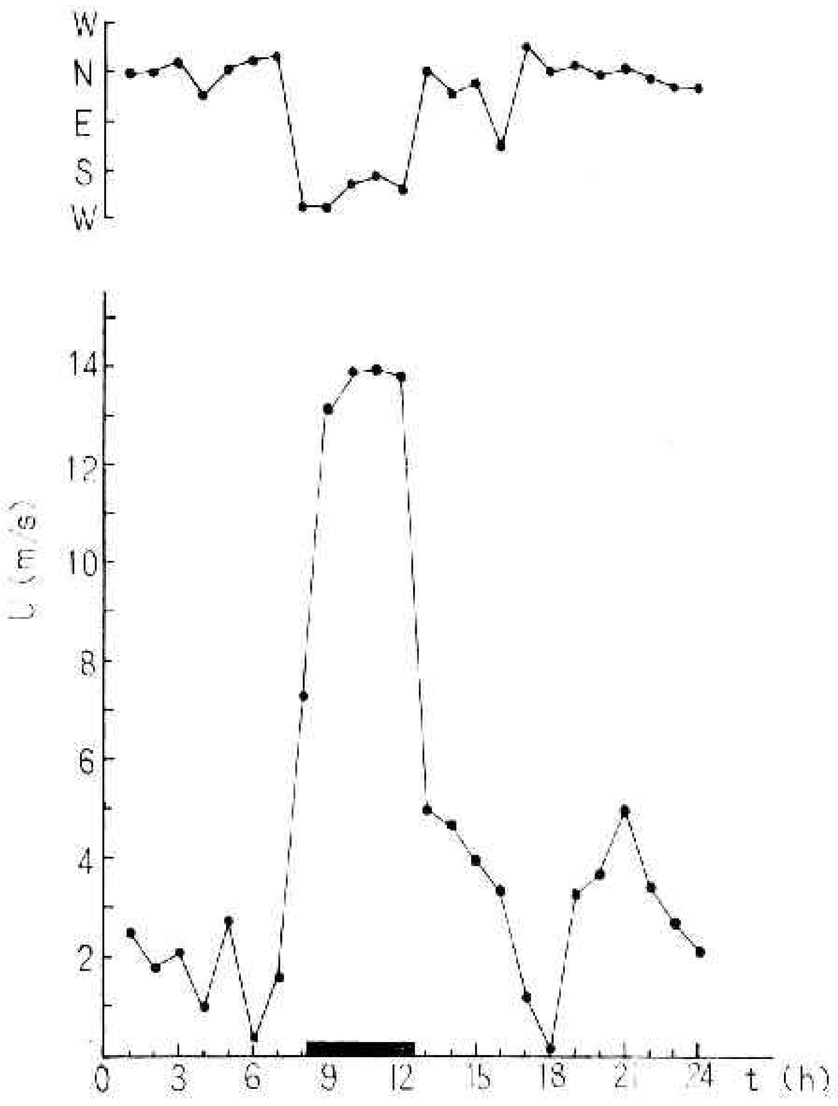

(3) 26 December 1969

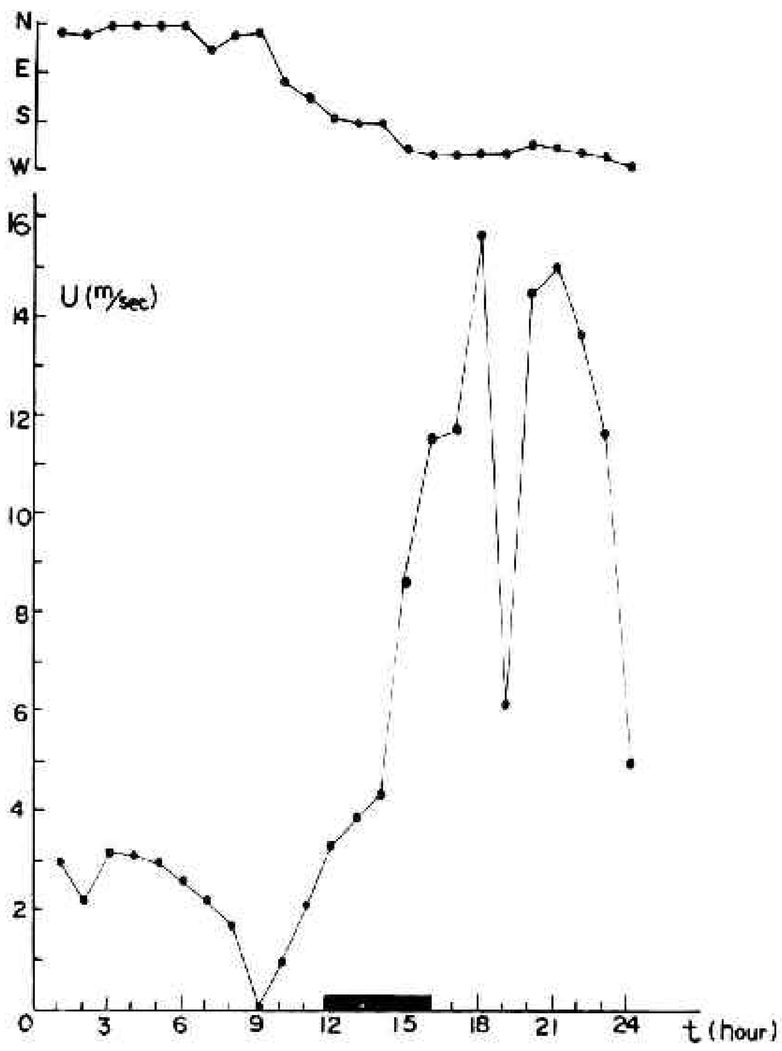

(4) 13 February 1970

Fig. 1. 1 Mean wind velocity and duration, the interval of observation being thickened on the abscissa.

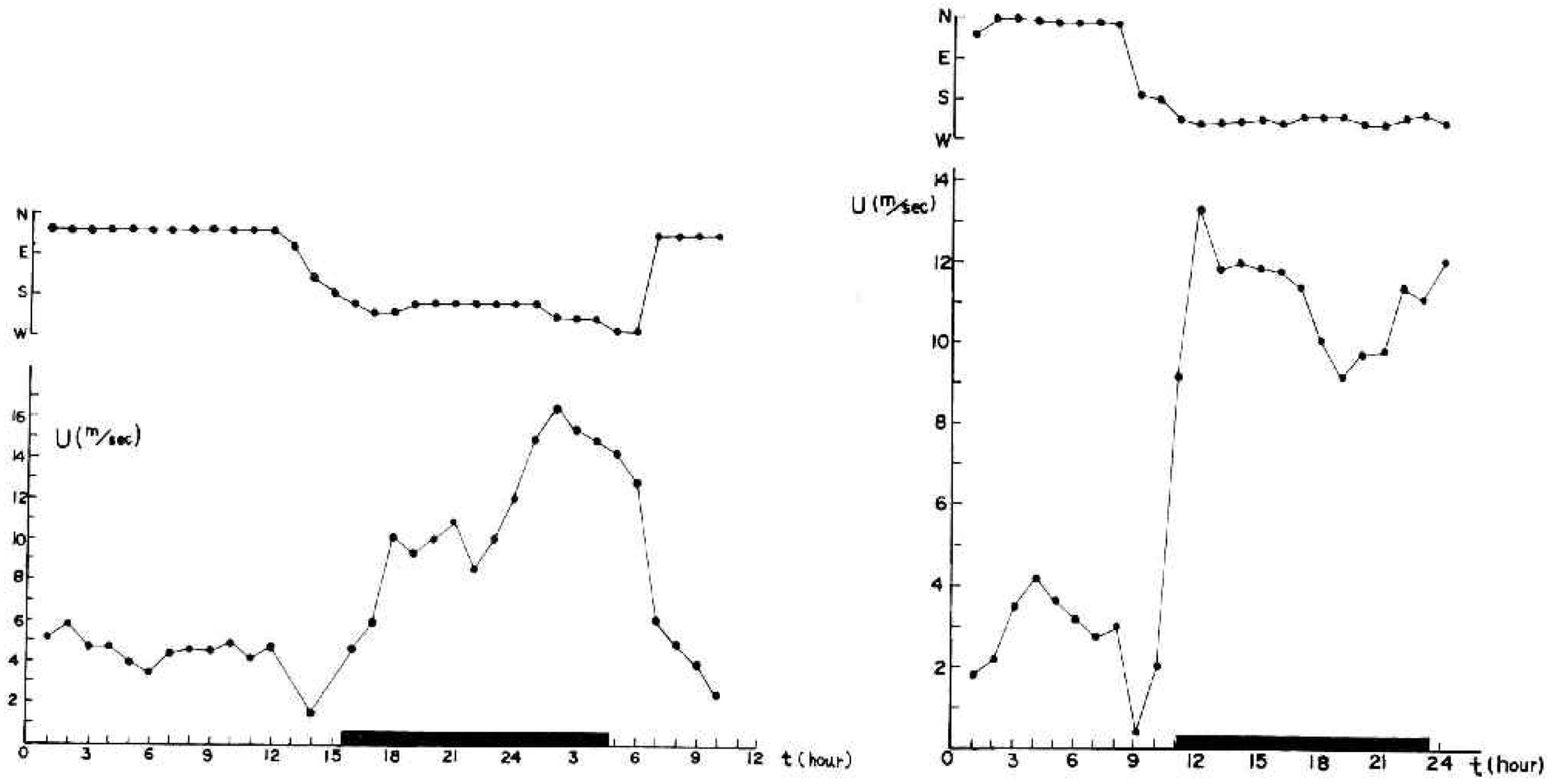

(5) 20 February 1970　　(6) 10 November 1970

Fig. 1. 2 Mean wind velocity and duration, the interval of observation being thickened on the abscissa.

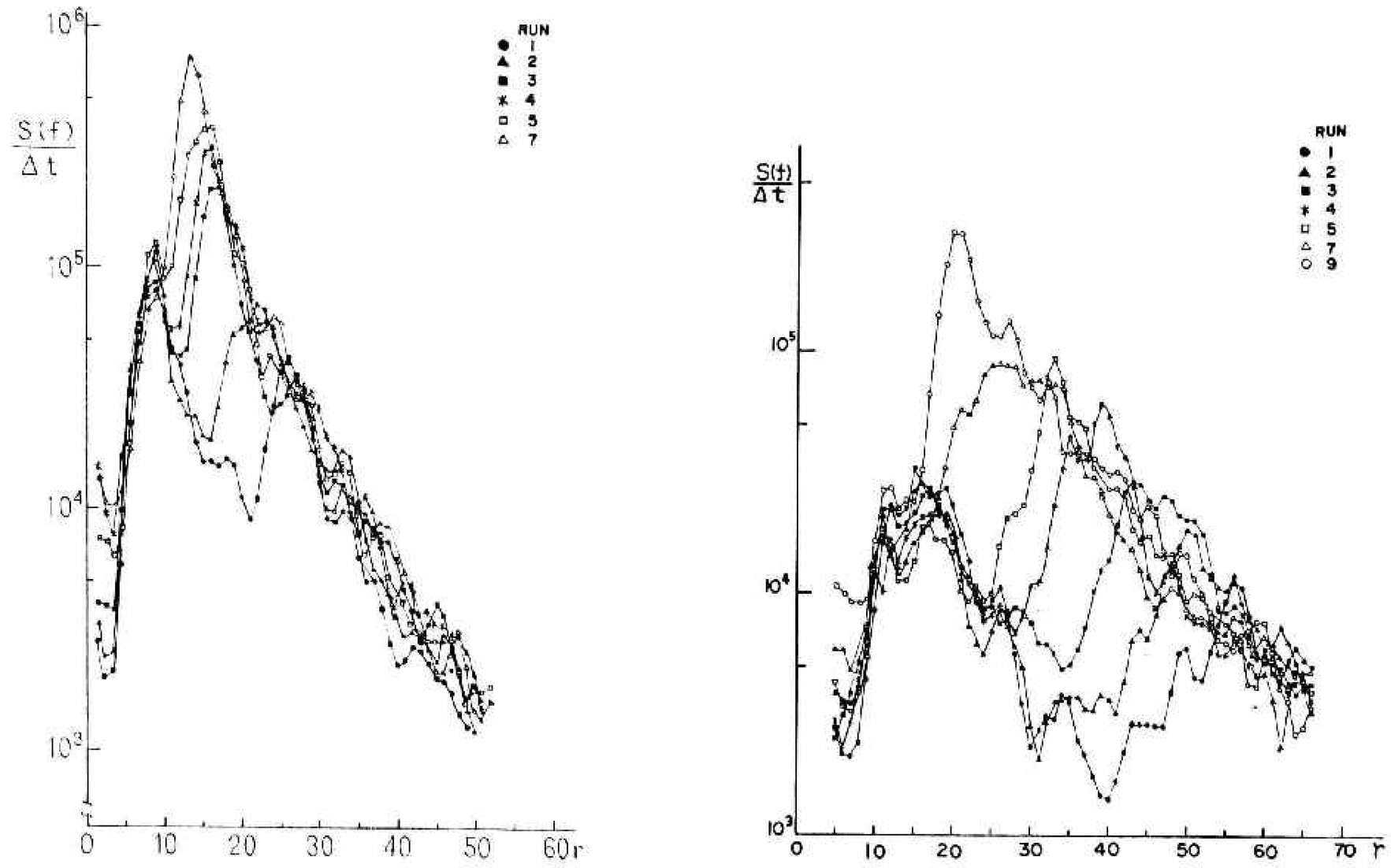

(1) 8 April 1969　　(2) 12 April 1969

Fig. 2. 1 Raw spectra in the developing stage.

2. Processing of data

All the following data are acquired at the Marine Observation Tower of Hiratsuka Branch, built at the spot of 20-m depth, 1.3 km offshore.

Figs. 2(1)—2(6) show the general characteristics of power spectra in transient stages, and the unit of ordinate is arbitrary and the abscissa must be read as

$$f=\frac{r}{2\Delta tH},$$

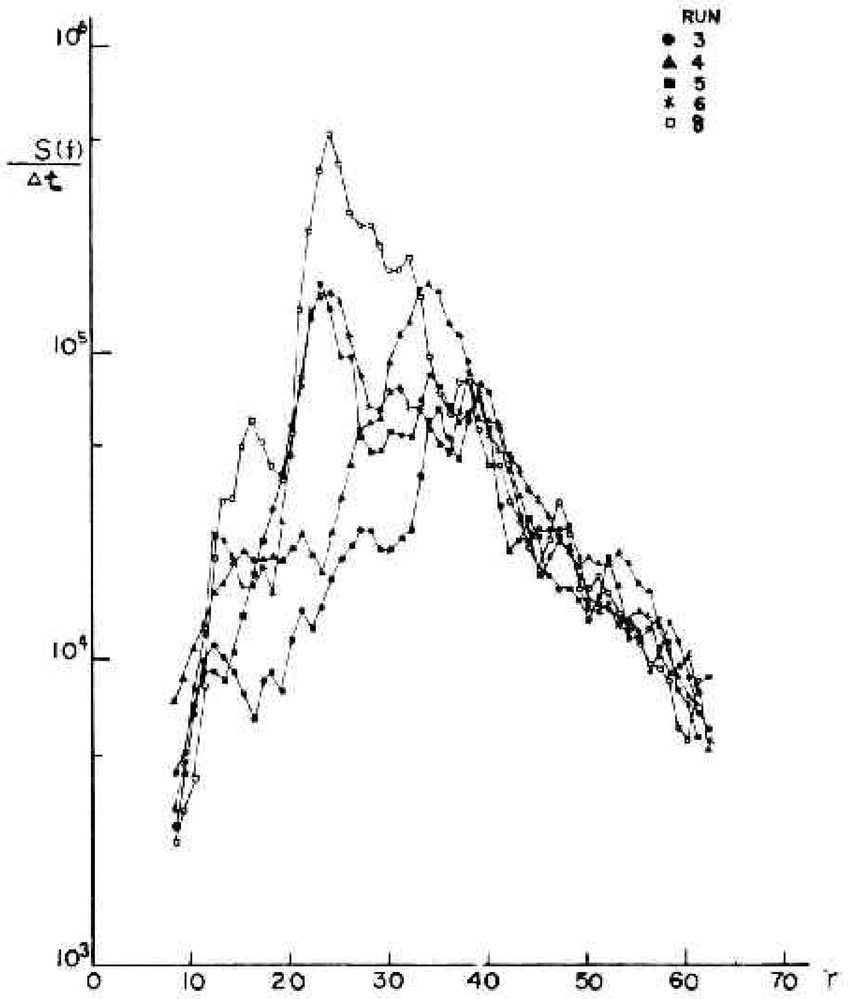

(3) 26 December 1969

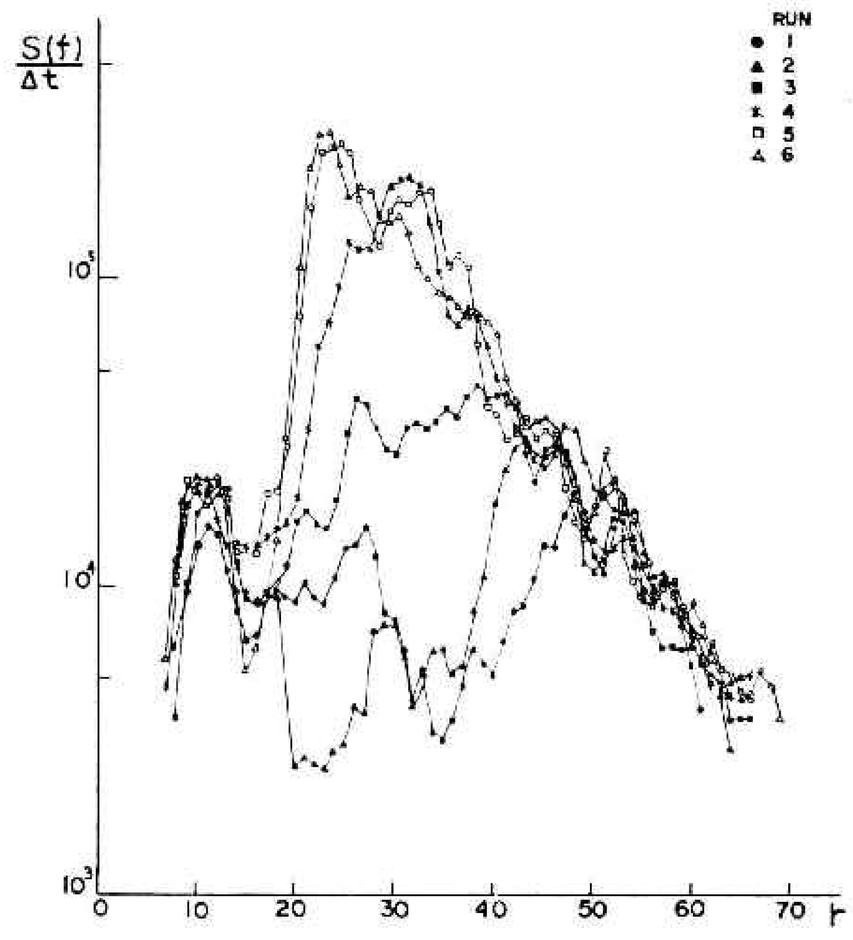

(4) 13 February 1970

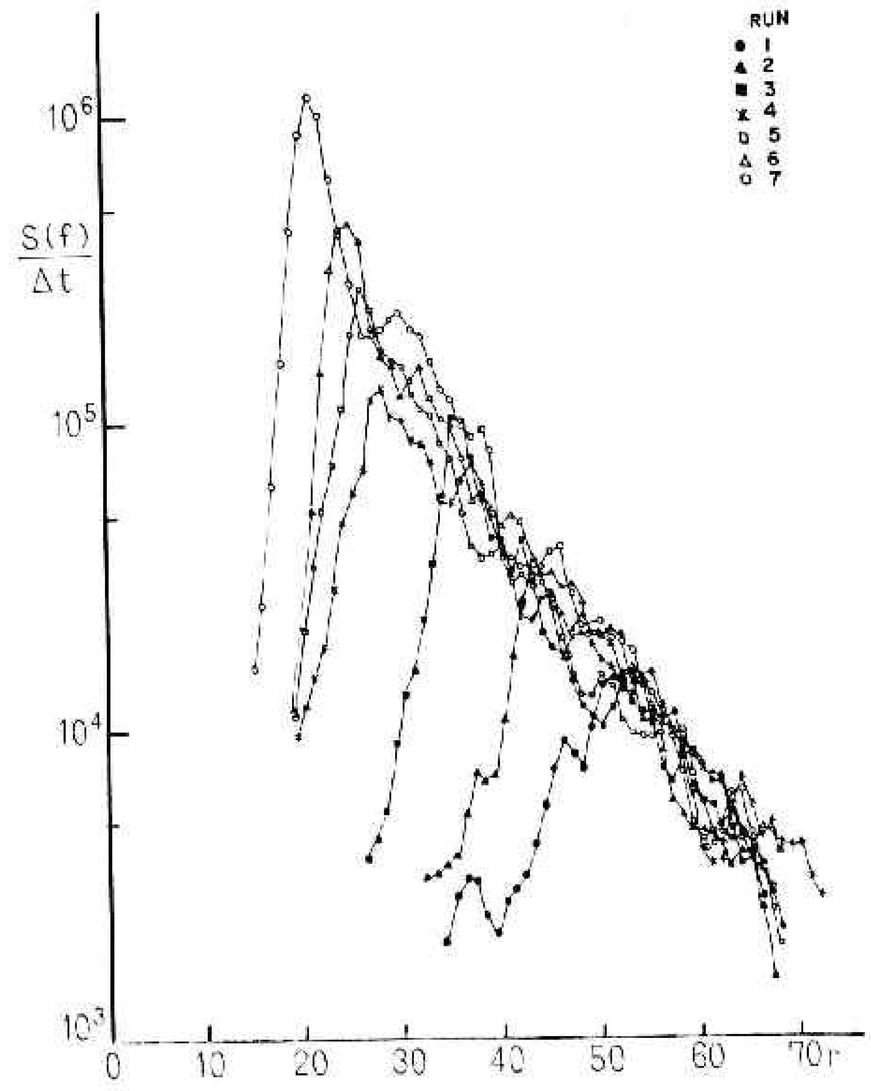

(5) 20 February 1970

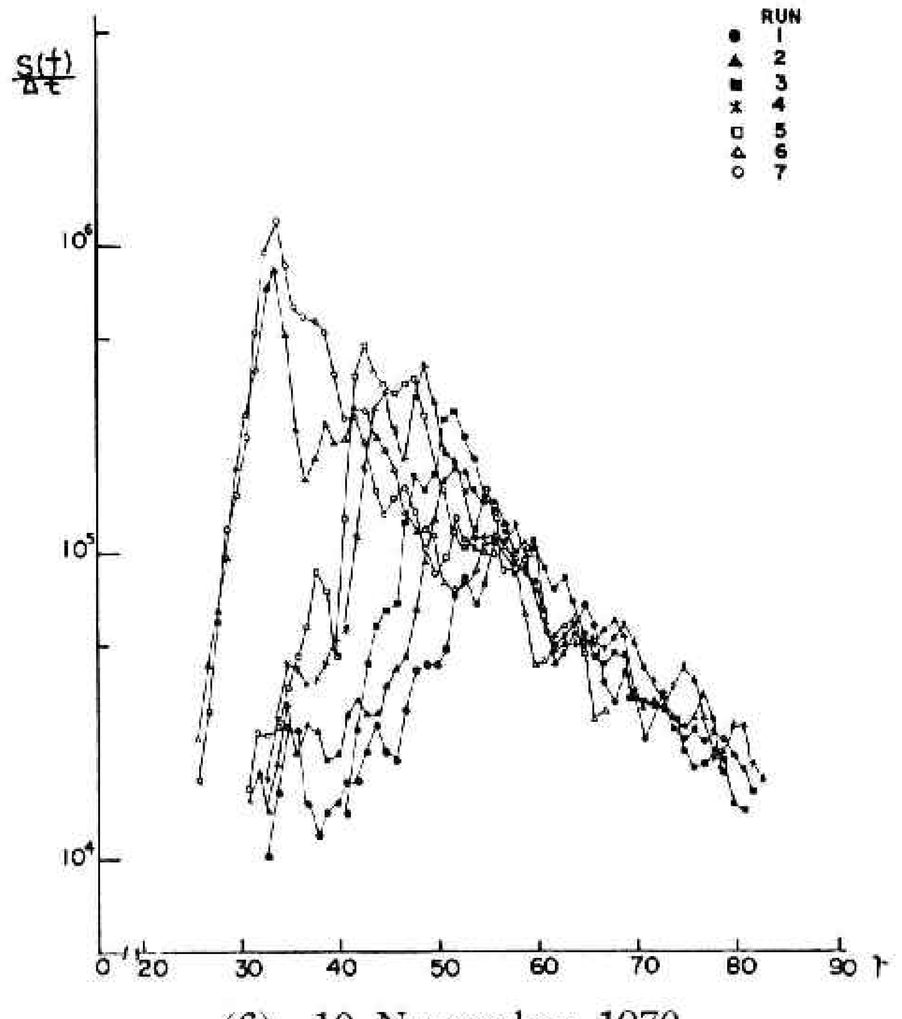

(6) 10 November 1970

Fig. 2. 2 Raw spectra in the developing stage.

where Δt: sampling interval of data acquisition, H: lag number of spectrum. Each set of observations is composed of several successive runs, whose agenda are given in Tables 1—6.

The variations of wind field are shown in Figs. 1(1)—1(6). The most predominant feature of these raw spectra is the displacement of the optimum frequency of spectra towards the low frequency range, according as the duration of wind increases.

Figs. 3(1)—3(6) show normalized spectra corresponding to (10). Except in Figs. 3(3) and 3(6), normalized spectra are not similar to each other. The slope of the spectrum in the higher frequency range is somewhat larger in the initial

Table 1. 8 April 1969.
($\Delta t=0.3$, $H=100$)

Run	Time h m	r_m	T_m sec	$T_{1/3}$ sec	$H_{1/3}$ cm
1	10 20	25	2.40	5.46	36.08
2	40	21	3.00	4.82	44.80
3	11 00	17	3.51	4.72	55.12
4	20	16	3.71	4.81	64.58
5	40	15	4.00	4.70	74.89
6	12 00	14	4.29	4.91	90.24
7	40	15	4.00	4.74	74.08
8	13 00	12	5.00	5.05	100.41

Table 2. 12 April 1969.
($\Delta t=0.6$, $H=100$)

Run	Time h m	r_m	T_m sec	$T_{1/3}$ sec	$H_{1/3}$ cm
1	10 30	56	2.14	5.91	31.02
2	50	50	2.40	5.37	33.40
3	11 30	43	2.79	4.66	41.15
4	50	39	2.04	4.69	47.77
5	12 10	33	3.64	4.44	54.99
6	30	34	3.53	4.65	60.62
7	50	26	4.60	5.17	67.48
8	13 10	21	5.71	5.70	83.05
9	30	20	6.00	5.86	90.74

Table 3. 26 December 1969.
($\Delta t=0.6$, $H=100$)

Run	Time h m	r_m	T_m sec	$T_{1/3}$ sec	$H_{1/3}$ cm
1	8 15			4.26	65.67
2	55			4.24	62.69
3	9 35	39	3.08	4.16	58.84
4	10 15	34	3.53	4.35	77.96
5	55	24	5.00	4.17	75.18
6	11 35	24	5.00	5.01	78.75
7	55			5.14	89.79
8	12 15	24	5.00	5.23	117.89

Table 4. 13 February 1970.
($\Delta t=0.6$, $H=100$)

Run	Time h m	r_m	T_m sec	$T_{1/3}$ sec	$H_{1/3}$ cm
1	11 55	48	2.50	4.68	36.31
2	12 15	47	2.76	4.11	43.52
3	35	38	3.16	4.60	56.16
4	55	31	3.87	4.83	91.28
5	13 15	24	5.00	5.23	106.22
6	35	23	5.22	5.31	103.40
7	15 55	22	5.45	5.56	120.04

Table 5. 20 February 1970.
($\Delta t=0.6$, $H=100$)

Run	Time h m	r_m	T_m sec	$T_{1/3}$ sec	$H_{1/3}$ cm
1	15 34	52	2.31	9.13	17.21
2	17 34	44	2.72	5.05	30.34
3	18 34	36	3.33	4.54	38.58
4	19 34	28	4.28	4.26	54.35
5	21 34	26	4.61	4.77	71.53
6	24 34	25	4.81	5.02	93.43
7	4 34	21	5.71	5.02	87.79

Table 6. 10 November 1970.
($\Delta t=1.0$, $H=100$)

Run	Time h m	r_m	T_m sec	$T_{1/3}$ sec	$H_{1/3}$ cm
1	11 15	56	3.58	5.16	77.16
2	40	51	3.92	4.87	92.33
3	12 05	51	3.92	4.78	102.17
4	14 30	48	4.16	5.06	118.87
5	15 45	42	4.76	5.38	128.57
6	22 40	33	6.06	6.42	148.78
7	23 30	33	6.06	6.47	170.84

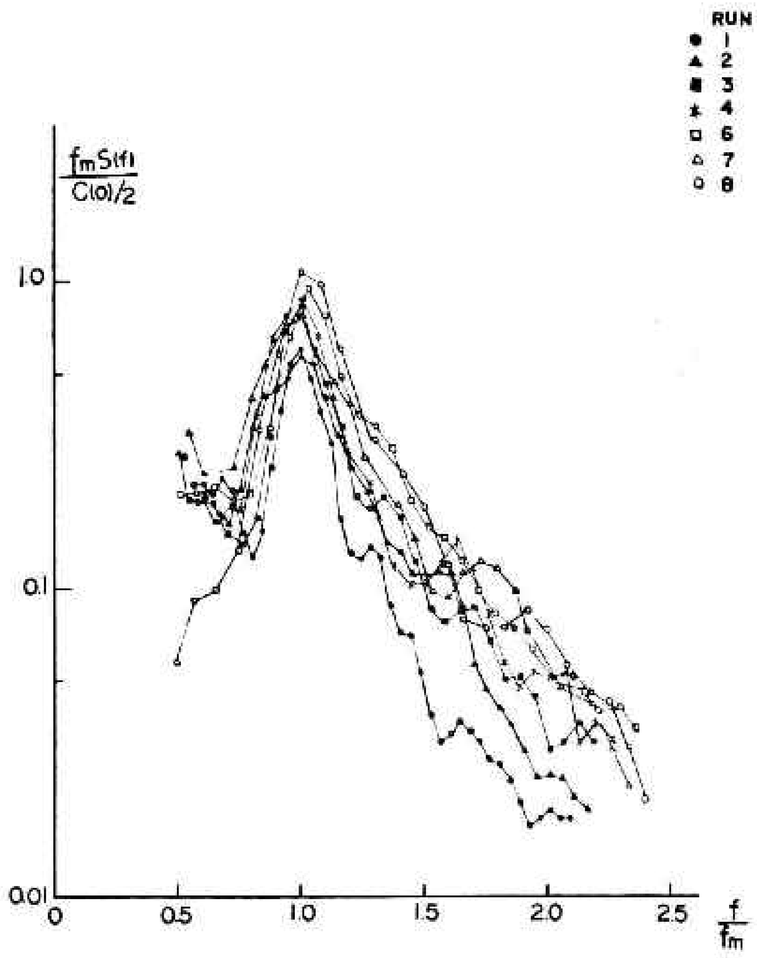

(1) 8 April 1969

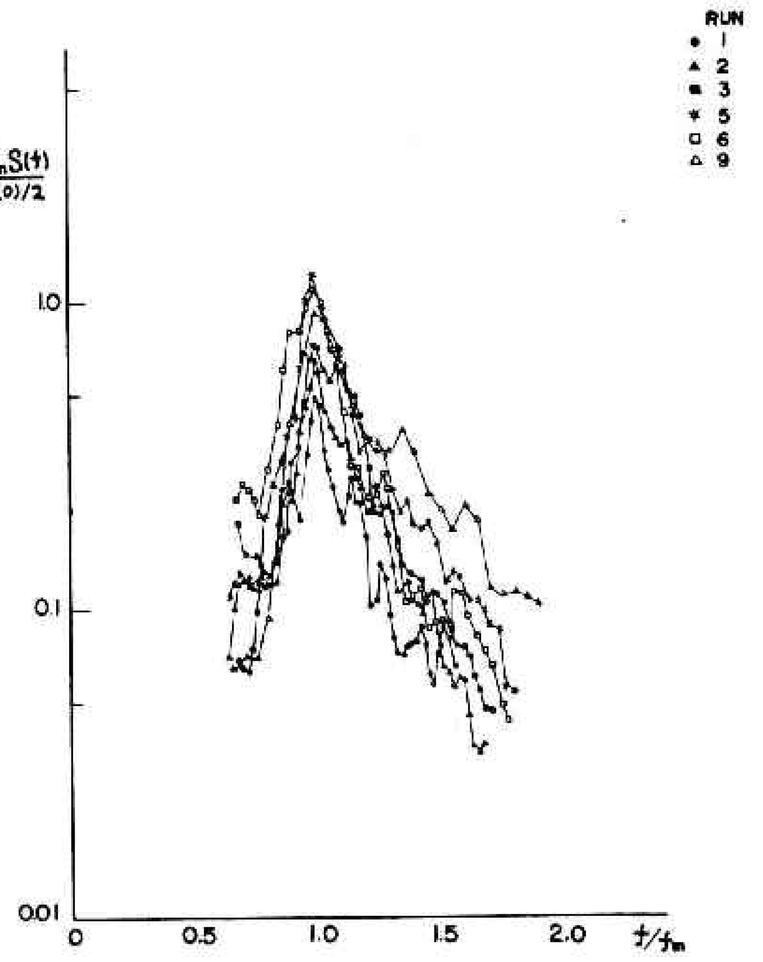

(2) 12 April 1969

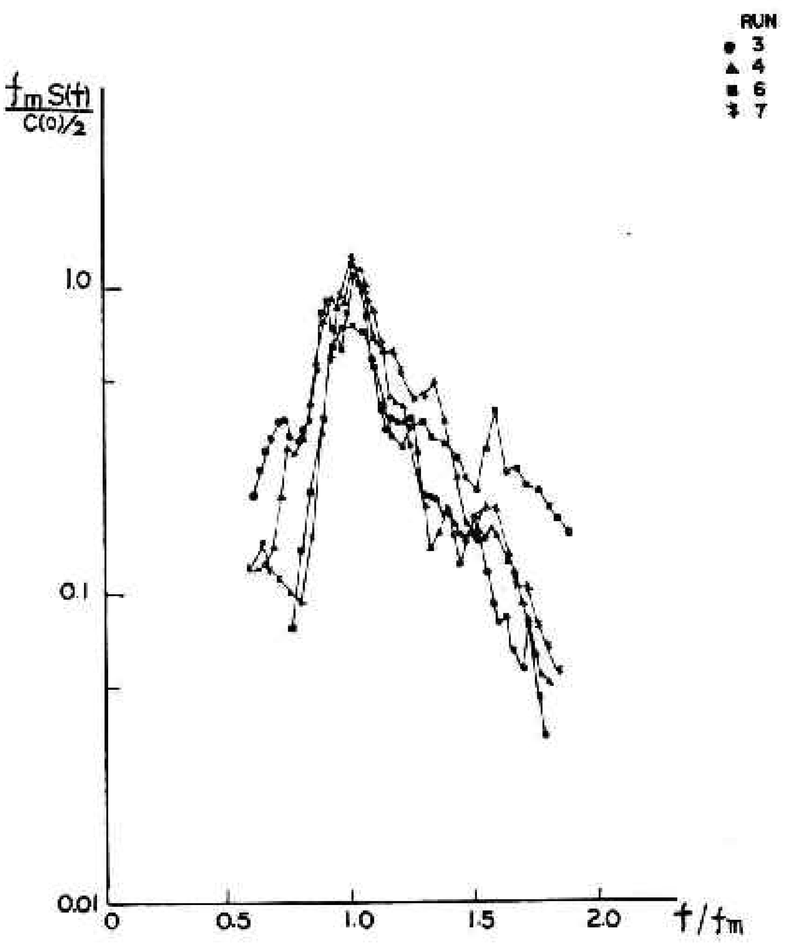

(3) 26 December 1969

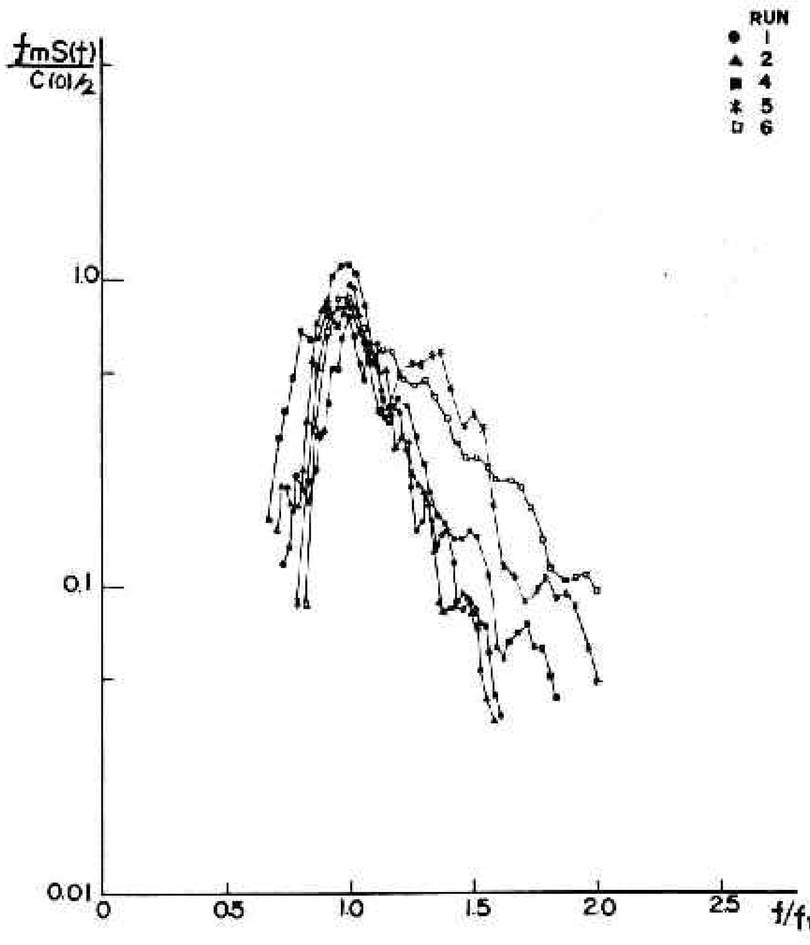

(4) 13 February 1970

Fig. 3. 1 Normalized spectra in the developing stage.

stage of the development than in the later stages. This is seen more accurately in Figs. 4(1)—4(6) plotted in logarithmic scale. Except in Figs. 4(3) and 4(6), each of the spectra in the higher frequency range has a slope larger than −5th power of frequency in the initial stage of development. Such spectra are rather assimilated as −6th power of frequency.

Figs. 4(3) and 4(6) show that all the spectra have similar slopes of the order of −5th power. Corresponding to them, we can see in Figs. 2(3) and 2(6) that there are rather large spectrum densities already from the first stage of observation. Optimum periods of the first run for these exceptional cases are respectively 3.1 sec and 3.6 sec as seen in Tables 3 and 6. For the cases other than these, on the contrary, they are smaller than 3.0 sec.

The reason of this discrepancy in the similarity form in the equilibrium range is not accurately known.

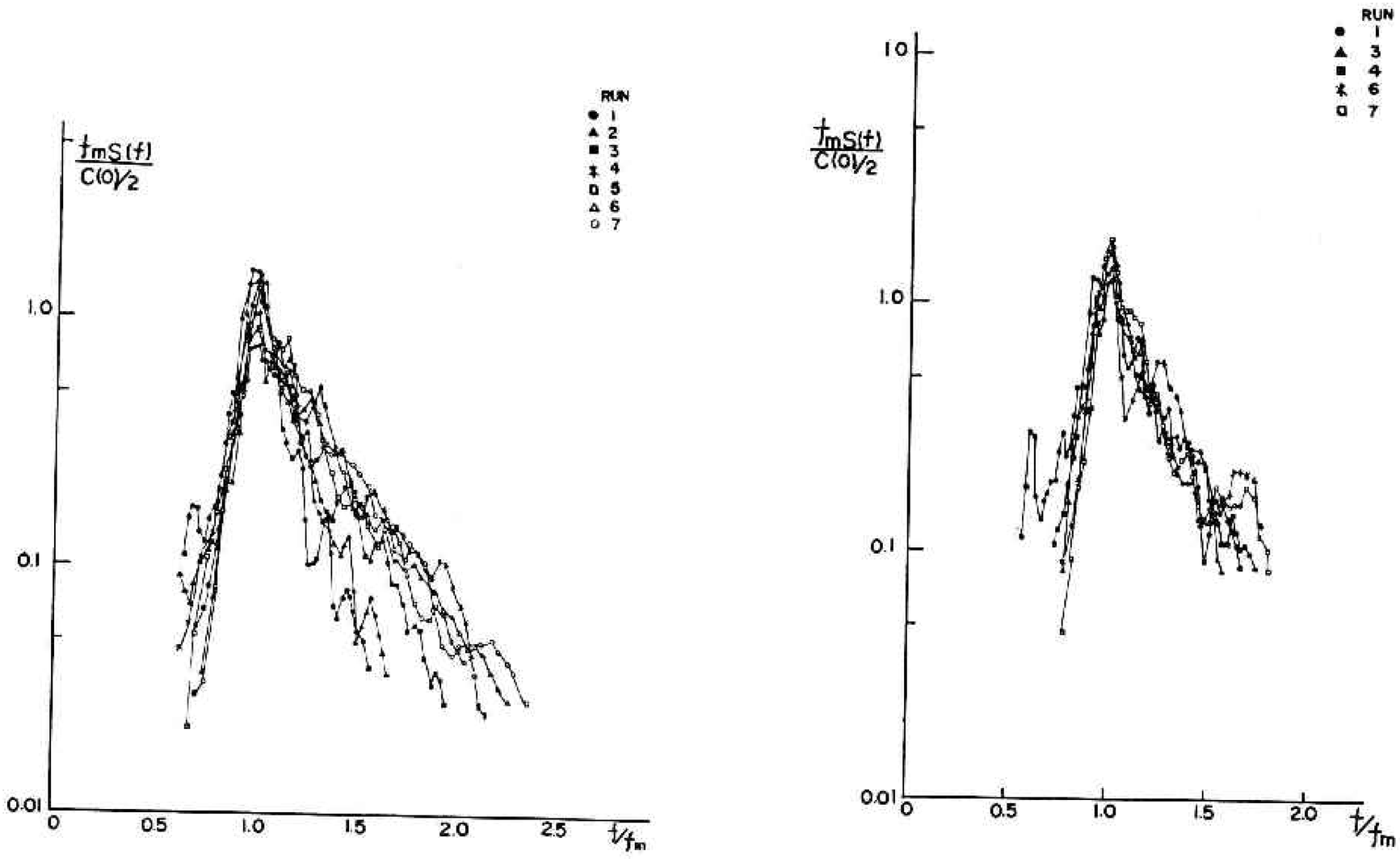

(5) 20 February 1970 (6) 10 November 1970

Fig. 3. 2 Normalized spectra in the developing stage.

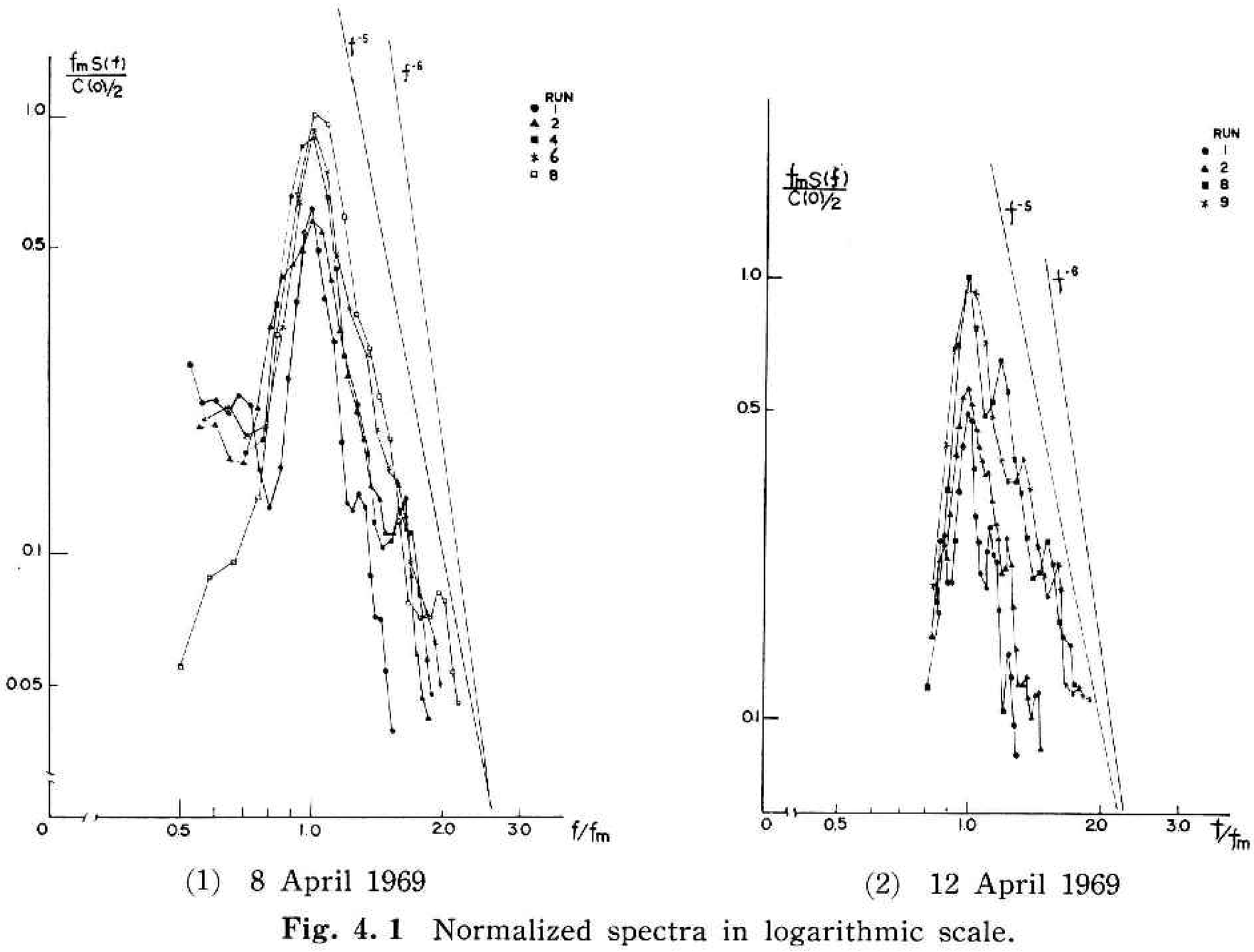

(1) 8 April 1969 (2) 12 April 1969

Fig. 4. 1 Normalized spectra in logarithmic scale.

One possible cause is the apparent distortion of surface displacement with higher frequency due to a delay in drainage as the water falls along the capacitance wave probe. This results in the decrease of the gain as frequency increases, so that the slope of the spectrum density becomes steeper. When we assume broadly this delay of water drainage as $\exp(-t/\tau)$, then we obtain roughly $\tau=1$

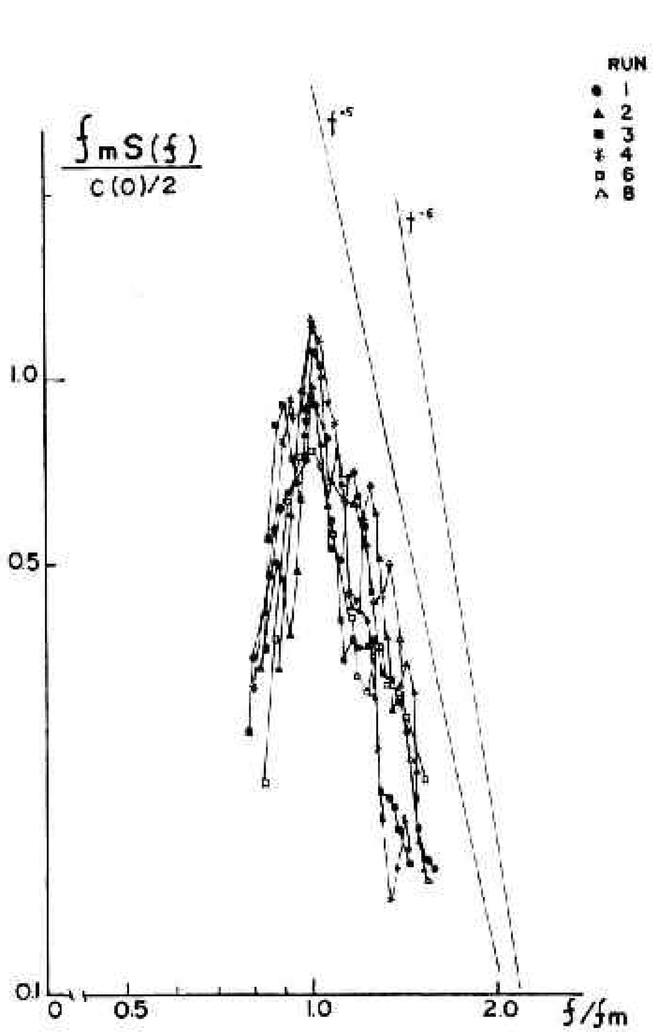

(3) 26 December 1969

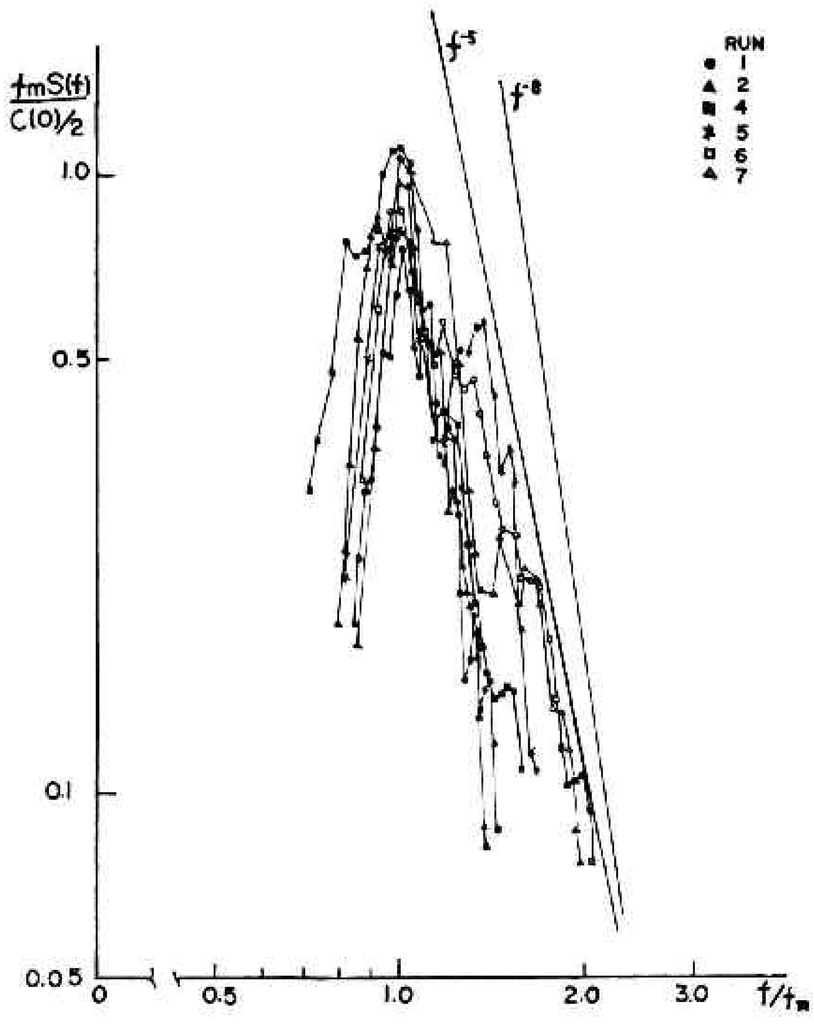

(4) 13 February 1970

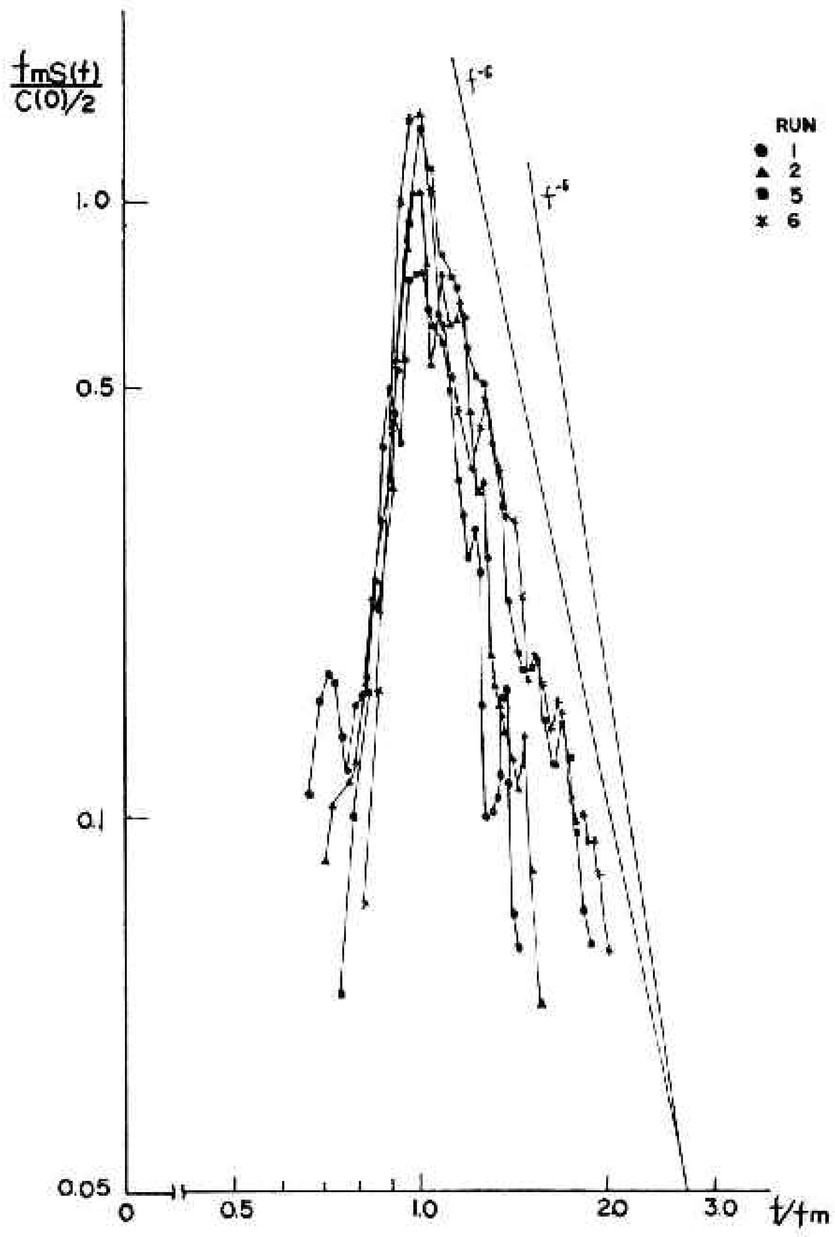

(5) 20 February 1970

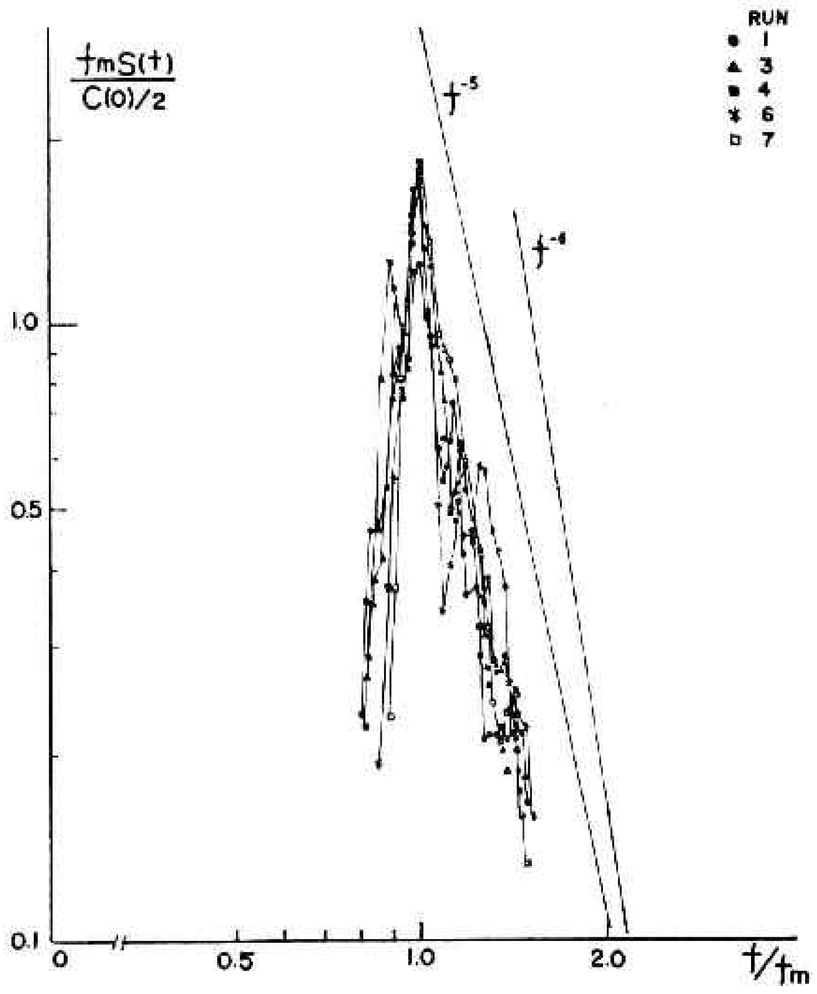

(6) 10 November 1970

Fig. 4. 2 Normalized spectra in logarithmic scale.

to 1.5 sec which is rather critical for our initial stage of development.

The other possible reason is the effect of induced current by wind in the early stage of development. From the energy conservation of wave field, we have from Phillips (1966, p. 60) the relation

$$E(\sigma)c(c+2U)\mathrm{d}\sigma=\text{constant}=E_0(\sigma_0)c_0^2\mathrm{d}\sigma_0\,, \tag{11}$$

where $c=g/\sigma$ and $c_0=g/\sigma_0$ are the local phase velocities, and U the mean current

speed, so that we have

$$\sigma_0=\sigma+kU=\sigma\left(1+\frac{\sigma U}{g}\right) . \tag{12}$$

After differentiation of (12) with σ and after substitution of them into (11), we have

$$E(\sigma)=\left(1+\frac{\sigma U}{g}\right)^{-2} E_0(\sigma_0).$$

When the power spectrum of surface waves for the case of still water is given by

$$E_0(\sigma_0)=\beta g^2\sigma_0^{-5} ,$$

then the above relation can be written as follows:

$$E(\sigma)=\beta g^2\sigma^{-5}\left(1+\frac{\sigma U}{g}\right)^{-7} ,$$

which shows that the level of spectrum density decreases more rapidly than for the case of still water.

It is interesting to note that the same rapid decrease of power density in the higher frequency range is always observed in the wind-water tunnel experiment conducted by Hamada (1966).

Acknowledgements:—The author wishes to thank Mr. O. Mashiko for his aid in numerical calculations and in preparation of figures.

References

1) Hamada, T. (1966): On the f^{-5} law of wind-generated waves. *Rep. Port and Harbour Res. Inst.*, No. 12.
2) Kitaigorodski, S.A. (1961): Applications of the theory of similarity to the analysis of wind-generated wave motion as a stochastic process. *Izv., Geophys. Ser.*, 105-117.
3) Mitsuyasu, H. (1968): On the growth of the spectrum of wind-generated waves (I). *Rep. Kyushu Univ.*, XVI, No. 55.
4) Mitsuyasu, H. (1969): On the growth of the spectrum of wind-generated waves (II). *Rep. Kyushu Univ.*, XVII, No. 59.
5) Phillips, O.M. (1958): The equilibrium range in the spectrum of wind-generated waves. *J. Fluid Mech.*, **4**, 426-434.
6) Phillips, O.M. (1966): *The dynamics of the upper oceans.* Cambridge Univ. Press, pp. 261.

(Manuscript received 10 May 1971)

発達過程にある風浪のスペクトルの相似性

岩　田　憲　幸

国立防災科学技術センター平塚支所

平塚支所の波浪等観測塔で，南の風が突然吹き出したときの波浪の発達を，容量型波高計で観測しスペクトル解析を行なった．観測期間中の極大周期は 6 秒を越えたものはない．6 秒の波の群速度は 18 km/h であるから相模灘で風が吹き出してからの数時間は，吹送距離は無限大とみなしてさしつかえない．極大周波数と分散とで無次元化したスペクトルを求めると，風の吹き始めの，1～2時間を除くと，スペクトルは相似になる．最初のスペクトルでは，高周波側の傾斜が周波数の −5 乗より強く，−6 乗ぐらいになる．その理由は明らかでないが，考えられることのひとつは，波高計プローブの水切りが悪く高周波側で利得が落ちることであり，いまひとつの原因は，風の吹き出しによって生じる吹送流によるものと思われる．